A novel tandem route to renewable isoprene over Mo-Fe oxide and mesoporous Cu/MgO composite catalysts

Lulu Xu [a], Shuo Liu [a], Xiangju Meng [b], Feng-Shou Xiao [c], Trees De Baerdemaeker [d], Andrei-Nicolae Parvulescu [d], Bernd Marler [e], Ute Kolb [f], Dirk De Vos [g], Toshiyuki Yokoi [h], Weiping Zhang [a,*]

[a] State Key Laboratory of Fine Chemicals, School of Chemical Engineering, Dalian University of Technology, Dalian 116024, China
[b] Department of Chemistry, Zhejiang University, Hangzhou 310028, China
[c] College of Chemical and Biological Engineering, Zhejiang University, Hangzhou 310027, China
[d] BASF SE, Process Research and Chemical Engineering, 67056 Ludwigshafen, Germany
[e] Institute für Geologie, Mineralogie und Geophysik, Ruhr-Universität Bochum, Germany
[f] Institut für Physikalische Chemie, Johannes Gutenberg-Universität Mainz, 55128 Mainz, Germany
[g] Center for Surface Chemistry and Catalysis, K. U. Leuven, Leuven, Belgium
[h] Institute of Innovative Research, Tokyo Institute of Technology, Yokohama 226-8503, Japan

ARTICLE INFO

ABSTRACT

The preparation of renewable isoprene from biomass-derivable feedstocks is extremely desirable for the sustainable rubber/latex/pharmaceutical industries. We report here a novel tandem route to efficiently produce isoprene via bio-sourced methanol and isobutene over Mo-Fe-O+meso-Cu/MgO composite catalysts. High isoprene selectivity of 85 % was achieved at methanol conversion of 91 % under optimal conditions. Adding Cu into mesoporous MgO finely tunes the basicity and acidity balance, thereby promoting isoprene selectivity. It shows good recycle capability, with isoprene selectivity remaining 85 % after five successive regeneration cycles. *In-situ* DRIFTS of methanol and isobutene adsorption suggest the possible reaction pathways involve methanol oxidation to formaldehyde on Mo-Fe oxide, followed by Prins condensation between formaldehyde and isobutene to isoprenol, and final conversion to isoprene on meso-Cu/MgO. This work not only represents a great advance in industrial large-scale producing isoprene, but provides an efficient strategy for developing methanol as in-situ precursor of formaldehyde to participate in many reactions.

1. Introduction

Isoprene is an important raw material, with wide development and utilization in the rubber, latex, footwear and pharmaceutical industries [1–3]. Currently, isoprene is mostly obtained by the extraction of C_5 fraction, a by-product of ethene production [4]. However, this method is based on fossil fuel utilization, and is therefore detrimental to sustainability and environmental protection. Isoprene obtained via Prins condensation of formaldehyde and isobutene has received increasing attention from academia and industry owing to its simple process and a product with high purity [5]. This route is even more attractive in the sustainable chemical industry. The feedstock methanol, a precursor to formaldehyde, can also be derived from biomass [6,7]. Another feedstock isobutene can be directly gained from biomass [8] or from

dehydration of bio-based isobutanol [9]. Thus, it is a promising pathway for the production of renewable isoprene via Prins reaction, allowing to alleviate the dependence on petroleum.

Two processes can be used to produce isoprene namely, a two-step and a one-step processes [4,5,10,11]. The two-step process refers to the condensation of formaldehyde and isobutene first to 4,4-dimethyl-1, 3-dioxane (DMD) over acid catalyst, and then the vapor-phase decomposition of the formed DMD to isoprene over another acid catalyst [5]. This route suffers from complexity and economic losses. Compared to the two-step process, the one-step method is carried out in a fixed bed reactor and produces isoprene directly from formaldehyde and isobutene efficiently with lower energy requirements [4,11]. At present, the one-step process has been mainly carried out on acid catalysts such as zeolites [11], metal oxides [4], phosphate catalysts [12] and

heteropolyacid [13]. Unfortunately, these catalysts are prone to deactivation due to fast coke formation over acidic sites [14–16]. Zhu et al. reported the generation of carbon deposits covering strong acid sites over HZSM-5, thus improving the selectivity of isoprene at the expense of fast deactivation [16]. Ivanova et al. found that the presence of strong acidic sites benefited the formation of isoprene during the induction period, although the accumulation of carbon deposition led to a significant decline in formaldehyde conversion from 37 % to 15 % within 3 h over a Ni-Beta zeolite catalyst [15]. Furthermore, strong acidic sites lead to large amounts of aromatic and light hydrocarbons from the polymerization or cracking of isobutene [16–18]. Basic catalysts usually have stronger coke resistance since the coke formation is related to the acidic sites, and in many cases the modification of the acidic catalysts by base reduces the carbon deposits [19–21]. Basic catalysts have rarely been studied in this reaction. The potentially difficult problem for Prins condensation between formaldehyde and isobutene is the source of formaldehyde. Formaldehyde is typically obtained from formaldehyde aqueous solution or paraformaldehyde, for which the former requires catalysts with high water resistance [10] and the latter requires solvent dissolution [22]. In addition, formaldehyde is difficult to handle [23] with stringent transportation guidelines [24] owing to its low boiling point of −19.5 ℃. Formaldehyde is environmentally unfriendly and toxic [25] and at high concentrations will automatically polymerize to form a solid, leading to pipeline blockage, seriously affecting the process and causing huge economic losses [26]. Thus, taking all of the above adverse factors into account, it is urgent and necessary to find an alternative source for formaldehyde. In 1970′s Sumitomo chemical company reported CH_3OH and O_2 as the substitute of formaldehyde for Prins reaction over acidic catalysts such as H_3PO_4–MoO_3/SiO_2, Mo–Bi–P–Si oxides, etc. [27]. However, there may still be serious coke deposition on these acidic catalysts. Matsumoto et al. prepared isoprene from methanol and isobutene on supported silver catalysts [28], but its yield was quite low probably due to their reaction temperature of 280 ℃ was insufficient for the oxidation of methanol over silver catalysts. At present, formaldehyde is industrially produced by methanol oxidation in an air atmosphere over Ag-based catalysts at temperatures higher than 560 °C or over Mo-Fe-O catalysts at temperatures less than 400 °C [29, 30]. The synthesis of formaldehyde via methanol oxidation and the following Prins condensation with isobutene may be feasibly taken place in one pot, thereby avoiding storage and transportation of formaldehyde. Nevertheless, the key issue is to discover high-efficient catalysts for the entire reaction to make isoprene dexterously and also sustainably.

In this study, we report a novel tandem route to produce renewable isoprene using bio-sourced methanol and isobutene as feedstocks in a continuous mode under high pressure. Formaldehyde is formed in-situ via methanol oxidation over the Mo-Fe-O catalyst with redox sites. Then, the Prins condensation reaction between formaldehyde and isobutene to isoprenol takes place over acidic and/or basic sites, and finally, isoprenol is dehydrated to isoprene on the acidic sites. These three steps can be carried out on a composite Mo-Fe-O+acid/base catalyst loaded in a single fixed-bed reactor. We define this novel tandem route by the term "Oxidative Prins Reaction (OPR)" to distinguish it from the traditional Prins reaction. Our route provides many advantages such as skipping the reaction steps to minimize the operation complexity, and avoiding the use of aqueous formaldehyde and its handling challenges, which will be conducive to large-scale industrial production. Typical strong Brönsted solid acid such as HZSM-5, HBeta and HY zeolites, a Lewis acid such as γ-Al_2O_3, and basic catalysts such as MgO, CaO, and BaO were combined with Mo-Fe oxides and their catalytic performances were compared in detail in the oxidative Prins reaction. The reactivity correlation with basicity/acidity was investigated systematically under an oxidative atmosphere through CO_2-TPD, NH_3-TPD, methanol/CO_2 adsorbed FT-IR spectra and ^{1}H MAS NMR measurements after the adsorption of pyrrole and NH_3, respectively, as the probe molecule. The reaction network was also verified and described specifically by in-situ DRIFTS.

2. Experimental section

2.1. Catalyst preparation

The Mo-Fe-O catalysts were synthesized by the co-precipitation method. Commercial MgO (Tianjin Kermel, China) was used without further purification. Meso-MgO with a mesoporous structure was synthesized by the hydrothermal method. Meso-Cu/MgO catalysts with different Cu metal loadings were prepared by the impregnation approach. The detail information on the catalyst preparation was presented in the Supplementary Material.

Regeneration of the spent Mo-Fe-O+meso-Cu/MgO catalyst was carried out by calcination in air for 5 h at 440 °C for 2Mo-Fe-O pellets and 470 °C for meso-2 %Cu/MgO pellets.

2.2. Catalyst characterization

The molar ratios of Mo/Fe and the content of Cu over meso-Cu/MgO in the resulting catalysts were determined by inductively coupled plasma atomic emission spectroscopy (ICP-AES, Optima 2000 DV, USA). X-ray diffraction (XRD) analysis was carried out on an X-ray diffractometer (Rigaku D-Max Rotaflex) using Cu Kα radiation ($\lambda = 1.5418$ Å) with a scanning rate of 10°/min in the range of 2θ = 5–80° for the wide-angle part, and a scanning rate of 1°/min in the range of 2θ = 0.6–10° for the low-angle part. N_2 adsorption measurements were performed at −196 °C on a Micromeritics ASAP-2460 analyzer. Prior to the N_2 adsorption, the samples were evacuated at 623 K for 10 h. The surface area of the sample was calculated by the Brunauer-Emmett-Teller (BET) method. The density functional theory (DFT) method was used to calculate the pore size distribution (PSD) due to its more accuracy and reliability for irregular pore structures [31,32].

The CO_2-TPD, NH_3-TPD, and H_2-TPR experiments were all carried out on a micro fixed-bed reactor equipped with a mass spectrometer detector (Pfeiffer Omini-star, GSD-320). The pretreatment of samples and test details were listed in the Supplementary Material.

The adsorption of methanol or CO_2 followed by FT-IR as performed on a Thermo Fisher Nicolet iS10 spectrometer equipped with an environmental temperature chamber (PIKE Technologies). Methanol TPSR-MS was performed with a micro-reactor system connected to a mass spectrometer (Pfeiffer Omini-star, GSD-320). The pretreatment of samples and test details were listed in the Supplementary Material.

^{1}H MAS NMR experiments were performed on an Agilent DD2–500 MHz spectrometer with a 4 mm MAS probe at a spinning rate of 10 kHz. A π/4 pulse width of 1.1 µs and a recycle delay of 4 s were used, while the ^{1}H chemical shifts were referenced to trimethylsilane (TMS). For the ^{1}H MAS NMR measurements after the adsorption of pyrrole or NH_3, the samples were first subjected to thorough dehydration under vacuum at 400 °C for 24 h before adsorption. Then, sufficient pyrrole molecules were introduced into the activated samples at room temperature and were subsequently frozen by liquid N_2. Then, the samples were evacuated at 60 °C for 2 h to remove the physically-adsorbed pyrrole molecules. Finally, the samples were transferred to an NMR rotor sealed by a gas-tight endcap in an N_2-filled glove box. For the experiments with NH_3, the dehydrated samples were treated with a 1 % NH_3/N_2 flow at room temperature for 2 h, followed by heating under flowing He at 180 °C for 1 h to remove the physically adsorbed NH_3 and packed into NMR rotors in a glove box.

In-situ DRIFTS experiments were performed on a Thermo Fisher Nicolet iS10 spectrometer equipped with an environmental temperature chamber (PIKE Technologies). The pretreatment of samples and test details were listed in the Supplementary Material.
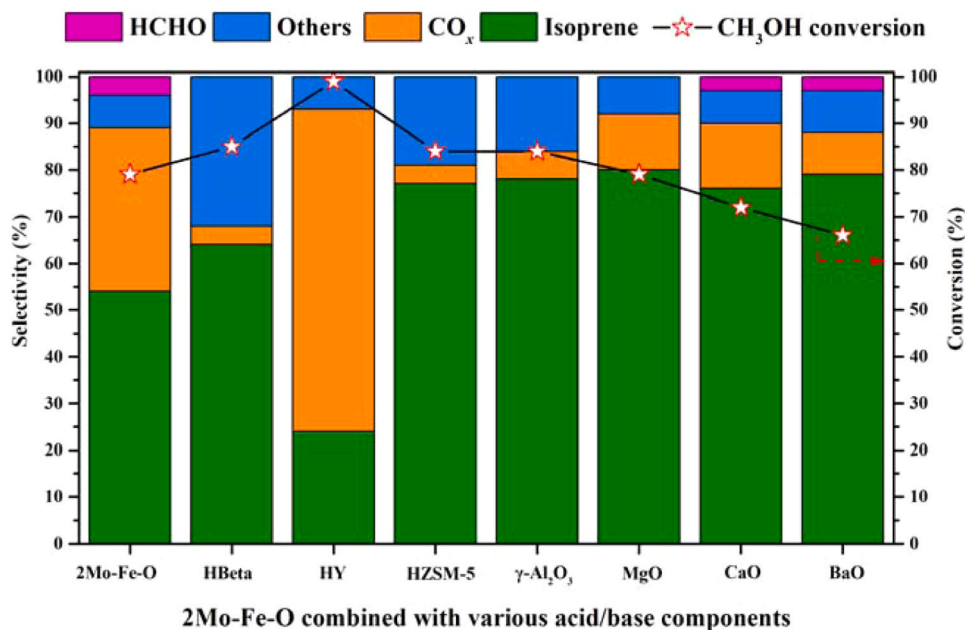
Fig. 1. Catalytic performances of 2Mo-Fe-O combined with various acid/base components for the oxidative Prins reaction of methanol and isobutene to isoprene. Reaction conditions: 240 ℃, 2.0 MPa, CH$_3$OH: Isobutene= 1:5, 15 % O$_2$/N$_2$, and 2.4 g$_{CH3OH}$/g$_{cat}$.h.

2.3. Catalytic reaction tests

The catalytic conversion of CH$_3$OH, O$_2$, and isobutene to isoprene was carried out in a high-pressure fixed-bed reactor (i.d. 10 mm). CH$_3$OH and isobutene were delivered to the high-pressure reactor filled with O$_2$/N$_2$ via a syringe pump, respectively, where the total flow rate was 30 mL/min. The products were analyzed by on-line GC (Shimadzu 2014 C) equipped with an FID detector plus a capillary OV1701 column (30 m, Zhonghuida Co. Ltd., China) and a TCD detector plus a packed GDX-403 column (2.5 m, Zhonghuida Co. Ltd., China). The conversion and selectivity were calculated on the basis of methanol since isobutene was taken in excess. Methanol was used as the bridge between FID and TCD for the selectivity calculation of HCHO and CO$_x$. More details on the reaction tests and performance analyses were given in the Supplementary Material.

3. Results and discussion

3.1. Oxidative Prins reaction performance over composite catalysts

The in-situ production of formaldehyde is the first step in the oxidative Prins reaction. Thus, the catalytic performance of methanol oxidation over the Mo-Fe-O catalysts was first investigated at high (2.0 MPa) or ambient pressure (0.1 MPa), and the results are shown in Fig. S1 (see Supplementary Material). Large amounts of CO$_x$ and minor amounts of HCHO were produced over all the Mo-Fe-O catalysts under high pressure. While high selectivity formaldehyde (ca. 86 %) was achieved on the 2Mo-Fe-O catalyst at ambient pressure. Therefore, 2Mo-Fe-O had the ability to produce HCHO with high selectivity although the as-generated HCHO was easily over-oxidized to CO$_x$ at high pressure because of the high surface oxygen coverages [33]. In addition, small amounts of CH$_3$OCH$_3$, (CH$_3$O)$_2$CH$_2$, and HCOOCH$_3$ were detected over the Mo-Fe-O catalysts [34,35]. High pressure leads to the over-oxidation of HCHO to CO$_x$, and also conduces to Prins condensation between HCHO and isobutene, indicating that these are two parallel and competitive reactions and the in-situ produced HCHO from methanol oxidation should undergo Prins condensation immediately to avoid over-oxidization. Prins condensation is typically catalyzed by acidic and/or basic sites, a balance of both is often considered to be the key

factor for driving selectivity [36]. Thus, the redox catalyst 2Mo-Fe-O and various acid/base components were combined to catalyze the oxidative Prins reaction between methanol and isobutene.

Fig. 1 summarizes the catalytic performances over the composite catalysts, while the detailed product distribution is shown in Table S1. 2Mo-Fe-O, without the addition of acid or base components, results in low selectivity of isoprene (~ 54 %), indicating that 2Mo-Fe-O could not only oxidize methanol to formaldehyde, but could also catalyze condensation between HCHO and isobutene owing to its own weak acidic/basic sites [37,38]. However, as shown in Fig. 1 and Table S1, the selectivity to CO$_x$ is 35 %, revealing that the acidity and basicity of 2Mo-Fe-O are not sufficient to favor the Prins condensation over the oxidation of HCHO, resulting in significant CO$_x$ production. In addition, ca. 4 % of HCHO, and minor amounts of (CH$_3$O)$_2$CH$_2$, CH$_3$OCH$_3$, and HCOOCH$_3$ were detected. When combined with different acid/base components, the product distribution especially the selectivity of isoprene and CO$_x$ varies significantly. Although the selectivity of CO$_x$ decreases significantly when combining 2Mo-Fe-O with HBeta and HZSM-5, the selectivity of isoprene improves slightly due to large amounts of other products formed over the strong Brönsted acid sites in line with previous results that strong acidic zeolites were less selective for isoprene in Prins condensation [16]. In addition, strong Brönsted acid sites would promote the protonation of isobutene, thus catalyzing the aromatization or cracking of isobutene [17,18]. The selectivities of other products decrease when 2Mo-Fe-O is combined with γ-Al$_2$O$_3$ with milder Lewis acid sites. This change in selectivity indicates that, although the acid sites are reported to be essential to improve the Prins condensation of HCHO and isobutene, the strength of these sites also plays a role in the eventual side reactions. A larger amount of CO$_x$ was detected when combining 2Mo-Fe-O with HY zeolite than other zeolites, which is possibly due to the cracking of isobutene caused by the stronger Brönsted acid sites and relative smaller diffusion resistance in HY zeolite since the cracking reaction is limited by diffusion in micropores [39]. When 2Mo-Fe-O is combined with basic metal oxides, the selectivity to CO$_x$ decreases dramatically with increasing selectivity to isoprene. In addition, the combination of basic metal oxides does not lead to the production of a large number of byproducts, since methanol conversion and isoprene selectivity are as high as 79 % and 80 %, respectively, over composite catalyst 2Mo-Fe-O combined with conventional MgO.
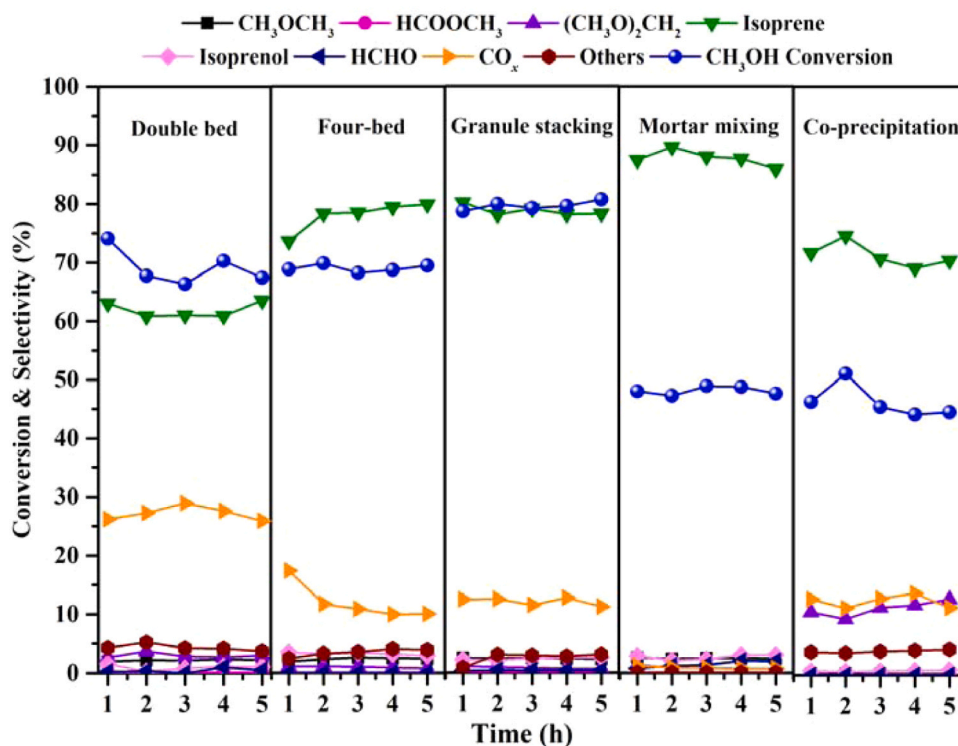
Fig. 2. Effect of the integration manner of 2Mo-Fe-O and MgO on the catalytic performances of methanol and isobutene to isoprene. Reaction conditions: 2Mo-Fe-O+MgO (1:1), 2.0 MPa, 240 °C, 15 % O_2/N_2, and 2.4 g_{CH3OH}/g_{cat}.h.

TG-DTG analysis of the combined catalysts after the reaction are displayed in Fig. S2(A-B). Compared with the peak intensity of weight loss in the TG profiles, the coke content reaches over 8 % on 2Mo-Fe-O combined with HY, HBeta, HZSM-5 or γ-Al₂O₃ because the acidic sites could easily lead to the formation of coke deposits [16]. While the coke content on 2Mo-Fe-O combined with basic metal oxides is less than 8 %. In addition, the DTG profiles reveal that strong acidic sites in zeolites also lead to the production of hard coke. Considering the catalytic performance and amount of coke deposition after the reaction, 2Mo-Fe-O+MgO was therefore selected as a potential composite catalyst for the following conversion of methanol and isobutene to isoprene.

3.2. Effect of the integration manner of the two active components

The effects of reaction temperature and pressure on activity were investigated over the 2Mo-Fe-O+MgO (1:1) catalyst (Fig. S3). Obviously, there is a large amount of residual formaldehyde at 0.1 MPa that has not undergone Prins condensation with isobutene, and as the reaction pressure increases from 0.1 to 2.0 MPa, negligible HCHO and high isoprene selectivity are observed, indicating that high pressure facilitates the condensation between formaldehyde and isobutene. Although high pressure caused severe over-oxidation of methanol to CO_x in the absence of isobutene (Fig. S1), it can promote the Prins condensation between formaldehyde and isobutene, which also inhibits the over-oxidation of formaldehyde in the presence of isobutene. Thus, 2.0 MPa was selected as optimum reaction pressure. We also optimized other reaction conditions on the 2Mo-Fe-O+MgO (1:1) catalysts for oxidative Prins reaction as shown in Figs. S4-S6. A methanol conversion of ∼ 79 % and isoprene selectivity of ∼80 % was achieved at optimal 2.0 MPa, 240 ℃, 15 %O_2/N_2, methanol/isobutene molar ratio of 1:5 and methanol WHSV of 2.4 g_{CH3OH}/g_{cat}.h.

As a tandem reaction, the product selectivity and distribution over the composite catalysts could be influenced by the integration manner of the active component [40–42]. The above results show that HCHO produced on 2Mo-Fe-O migrates rapidly to the surface of MgO, ensuring

condensation with isobutene rather than over-oxidation by 2Mo-Fe-O. 2Mo-Fe-O and MgO were mixed in separated beds (double and four-fold alternating beds), granule stacking bed, mortar mixing bed and further combined through co-precipitation method to examine the influence of the integration manner on catalytic performance. As depicted in Fig. 2, a large part of the formed HCHO was over oxidized into CO_x when the configuration of a double bed was applied, whereby MgO was loaded below 2Mo-Fe-O and separated by a layer of inert quartz sand. Notably, the relative selectivity of isoprene is as high as 80 %, and CO_x production is significantly suppressed at ca. 10 % selectivity when a four-fold bed is applied. Clearly, the noticeably high selectivity of isoprene again corroborates the bifunctional regime of this composite catalyst system on the oxidative Prins reaction. 2Mo-Fe-O and MgO combined in a granule stacking manner results in the enhancement of CH₃OH conversion to ca. 79 %, with similar selectivity to isoprene compared to the four-fold bed manner. These studies hint at the benefit of close proximity between 2Mo-Fe-O and MgO to obtain both high methanol conversion and isoprene selectivity. Furthermore, the 2Mo-Fe-O and MgO mixed by mortar mixing, which could be distributed with closer proximity, results in selectivity as high as 90 % for isoprene while total oxidation product CO_x is almost fully avoided. However, this integration manner leads to a decrease in methanol conversion from 79 % to 47 %, which indicates a detrimental effect on the redox sites of 2Mo-Fe-O. Furthermore, 2Mo-Fe-O and MgO could be distributed in closer proximity when they were combined through co-precipitation method. However, isoprene selectivity decreased drastically due to the formation of (CH₃)₂CH₂ and CO_x. According to the H₂-TPR results (Fig. S7) of the catalysts with different integration manners, mortar mixing and co-precipitation methods lead to overly intimate interactions between 2Mo-Fe-O and MgO, which possibly changes or weakens the oxidation ability of 2Mo-Fe-O. In this process, intimate interactions between 2Mo-Fe-O and MgO seem to have a synergistic effect, but the overly intimate interactions may weaken the oxidability of 2Mo-Fe-O. Thus, achieving appropriate proximity between the oxidation sites and the Prins condensation sites is the key to process
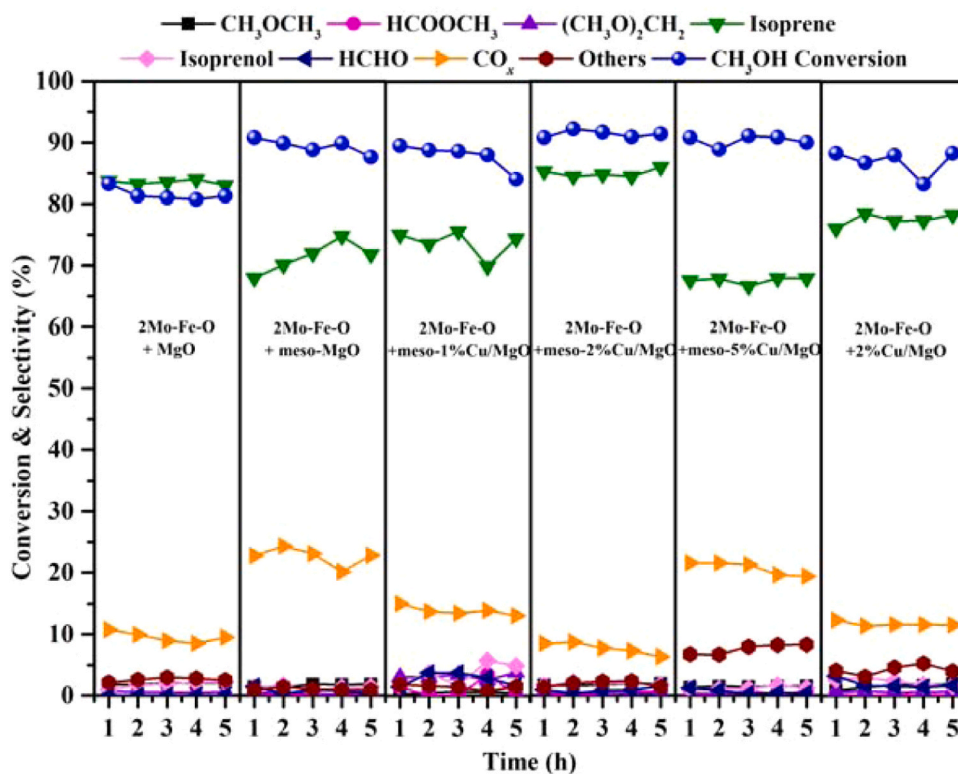
Fig. 3. Effect of the acidity and basicity of the catalysts on the catalytic performance of methanol and isobutene to isoprene. Reaction conditions: 2Mo-Fe-O+MgO (3:2), 2.0 MPa, 240 °C, CH_3OH: Isobutene= 1:5, granule stacking, 15 % O_2/N_2, and 2.4 g_{CH3OH}/g_{cat}.h.

optimization. Taking this into account, the effect of the 2Mo-Fe-O and MgO mass ratio on the performance was investigated as shown in Fig. S8. The excess amount of MgO in the composite catalysts results in methanol or HCHO decomposition to produce CO_x over the basic sites [35,43], while there is excess amount of 2Mo-Fe-O, there is an increase in oxidation sites, and generated HCHO is also easily oxidized to produce CO_x [35]. The balanced combination of 2Mo-Fe-O+MgO (3:2) shows excellent catalytic performance with 82 % methanol conversion and 83 % isoprene selectivity. These differences emphasize that the balance between oxidation sites and basic sites in the composite catalysts could improve the reaction performance.

The oxidation of methanol to formaldehyde over 2Mo-Fe-O is the first step in the oxidative Prins reaction. Isobutene has been also reported to be oxidized under a O_2 atmosphere over molybdenum-based catalyst [44–46]. To minimize the side reaction caused by isobutene oxidation, the isobutene oxidation reaction was analyzed during the entire oxidative Prins condensation. The results shown in Fig. S9 indicate that compared to the Prins condensation of isobutene, the reaction conditions selected herein allow to reduce the oxidation of isobutene almost completely.

3.3. Effect of the acidity and basicity on the catalytic performance

Modification of the basic sites on MgO could boost the Prins condensation between formaldehyde and isobutene. To investigate the effect of stronger basic sites (i.e., generation of isoprene), a series of catalysts with different basic properties were prepared to combine with 2Mo-Fe-O. The basic sites of MgO were previously modified by different synthesis conditions, while the generation of mesoporous structure possibly had strong basicity due to the formation of unsaturated oxygens [47,48]. Considering these results, we first synthesized meso-MgO with a mesoporous structure. As shown in Fig. 3, 2Mo-Fe-O+meso-MgO (3:2) shows ca. 24 % selectivity for CO_x, which is more than 2Mo-Fe-O+MgO (3:2). This result is unexpected since our original intention is to use

strong basic sites to catalyze Prins condensation between HCHO and isobutene; thus, inhibiting the over-oxidation of HCHO to produce CO_x. Basically, the generation of CO_x may come from both over-oxidation of HCHO and decomposition of methanol or HCHO. The over-oxidation of HCHO on 2Mo-Fe-O+MgO (3:2) could be the same on 2Mo-Fe-O+meso-MgO (3:2), since the redox properties of 2Mo-Fe-O in both the composite catalysts are the same. As discussed above, methanol or HCHO produced from methanol could be decomposed to produce CO_x over basic sites, while the presence of oxygen vacancies facilitates decomposition due to their strong basicity [35,43,49]. Thus, the increased selectivity of CO_x over 2Mo-Fe-O+meso-MgO (3:2) could possibly be caused by strong basic sites over meso-MgO rather than by 2Mo-Fe-O.

In general copper oxide was applied in many reactions as the mild Lewis acid sites [50]. Thus, Cu was introduced through impregnation method to prepare meso-Cu/MgO to modify the basicity and acidity balance in our study. As show in Fig. 3, the selectivity of CO_x over 2Mo-Fe-O+meso-Cu/MgO (3:2) decreases to values lower than 10 %, and isoprene selectivity increases to 85 % with increasing Cu content from 1 % to 2 %. This may be due to the decrease in basic strength of meso-MgO after modification by Cu. In addition, methanol conversion increases to about 91 % over 2Mo-Fe-O+meso-Cu/MgO (3:2) compared to 2Mo-Fe-O+MgO (3:2), possibly related to the acidic sites over the composite catalysts. As a comparison, we also evaluated the reaction performance of 2Mo-Fe-O+2 %Cu/MgO, where maybe the basic strength of MgO is insufficient to support Prins condensation after the addition of Cu, resulting in more CO_x produced through the over-oxidation of HCHO. This also shows the necessity of strong basic sites over 2Mo-Fe-O+meso-2 %Cu/MgO. However, Cu content of 5 % results in CO_x selectivity increasing to 20 %, and the others increase to about 9 % on 2Mo-Fe-O+meso-5 %Cu/MgO (3:2), leading to a decrease in isoprene selectivity. From the above results, it can be inferred that the presence of strong basicity over meso-MgO is not conducive to this reaction and the addition of an appropriate amount of Cu could modify the
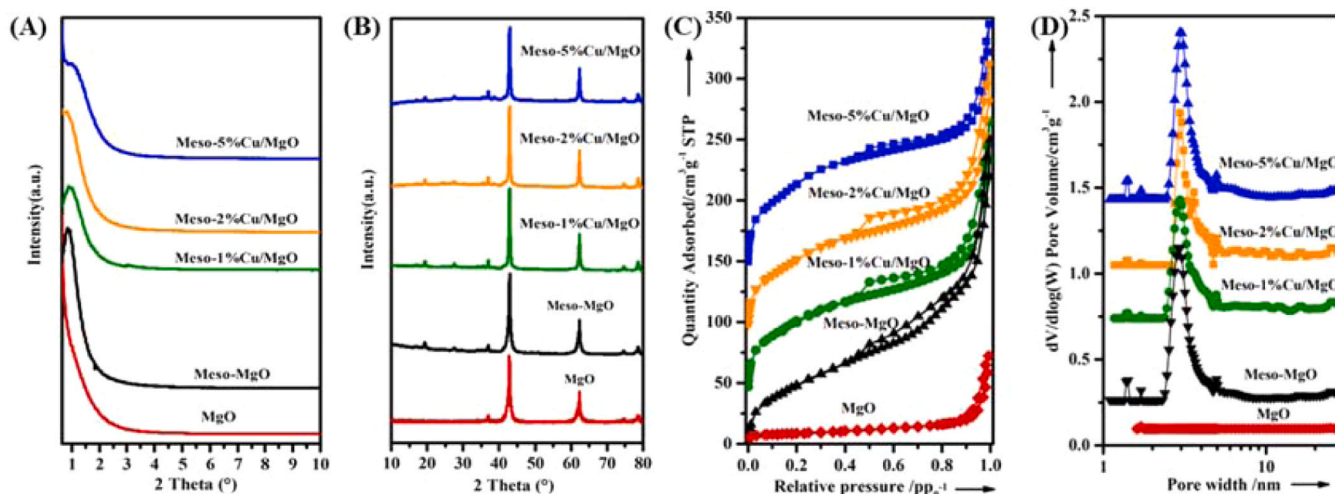
Fig. 4. (A) Low-angle XRD patterns, (B) wide-angle XRD patterns, (C) N_2 adsorption-desorption isotherms, and (D) Density-Function-Theory (DFT) pore size distribution (PSD) derived from the adsorption branches of the isotherms of the samples. The isotherms for meso-1 %Cu/MgO, meso-2 %Cu/MgO, and meso-5 %Cu/MgO were offset vertically by 50, 100 and 150 $cm^3 g^{-1}$, respectively. The PSD curves of meso-MgO, meso-1 %Cu/MgO, meso-2 %Cu/MgO and meso-5 %Cu/MgO were offset vertically by 0.3, 0.7, 1 and 1.4 $cm^3 g^{-1}$, respectively.

Table 1
BET surface areas, pore volumes and pore sizes of the Cu/MgO samples.

Sample	BET surface area (m^2/g)	Pore volume (cm^3/g)	Average mesopore size (nm)
MgO	53	0.12	-
Meso-MgO	211	0.34	2.9
Meso-1 %Cu/MgO	225	0.34	3.0
Meso-2 %Cu/MgO	200	0.33	2.9
Meso-5 %Cu/MgO	198	0.31	3.0

basicity and acidity, which is beneficial to the selectivity of isoprene and methanol conversion. We also investigated the oxidative Prins catalytic performance of meso-MgO and meso-2 %Cu/MgO without Mo-Fe-O. As shown in Fig. S10, the methanol conversions over both meso-MgO and meso-2 %Cu/MgO are very low, and it increases only less than 5 % after

introducing Cu. This demonstrates that the oxidation of methanol is almost negligible over copper oxide while it takes place readily over Mo-Fe oxide, which is an important step in oxidative Prins condensation. In addition, the converted methanol is decomposed to produce more CO_x on meso-MgO than on meso-2 %Cu/MgO, which may also indicate the addition of Cu tunes the basicity and acidity balance.

3.4. Catalysts characterization

3.4.1. XRD and N_2 adsorption

Fig. 4(A) shows the low-angle XRD patterns of the meso-MgO oxides with different Cu contents. The meso-MgO sample shows a distinct reflection peak centered at $2\theta = 1.0°$ and a minor peak appeared at $2\theta = 3.1°$, indicating that meso-MgO possesses a mesoporous framework [51]. With an increase in Cu content, the diffraction peak became weaker and broader and meso-5 %Cu/MgO gives only a small reflection peak at the low angle diffraction pattern, which indicates that the increase in Cu content is detrimental to the mesoporous framework of meso-MgO. The diffraction peaks at $2\theta = 36.9, 42.9,$ and $62.2°$

Table 2
Basic properties of the catalysts studied herein.

Catalysts	Total basic sites (µmol/g)[a]	Basic sites (µmol/g)[a]			Catalysts	Total[b]	Integrated Area (a.u.)[b]			ν_{CO} band integrated area per MgO mg for dissociated methanol (a.u.)[c]
		Weak	Middle	Strong			Unidentate carbonate	Bidentate carbonate	Bicarbonate species	
2Mo-Fe-O	17	0	0	17	-	-				
2Mo-Fe-O+MgO (3:2)	638	159	479	0	MgO	94	25	57	12	9.3
2Mo-Fe-O+meso-MgO (3:2)	972	245	470	257	Meso-MgO	105	40	55	10	11.3
2Mo-Fe-O+meso-1 % Cu/MgO(3:2)	779	289	328	162	Meso-1 % Cu/MgO	89	17	66	6	8.2
2Mo-Fe-O+meso-2 % Cu/MgO(3:2)	445	188	182	75	Meso-2 % Cu/MgO	64	6	55	3	7.5
2Mo-Fe-O+meso-5 % Cu/MgO(3:2)	185	81	86	18	Meso-5 % Cu/MgO	44	5	37	2	6

[a] measured by CO_2-TPD.
[b] All the integrated areas are given in arbitrary units as obtained from the deconvolution of the ν_{C-O} band between 1100 and 1900 cm^{-1} from CO_2-adsorbed IR spectra.
[c] All the integrated areas are given in arbitrary units as obtained from the deconvolution of the ν_{C-O} band of dissociative methanol at 1105 and 1085 cm^{-1} from methanol-adsorbed IR spectra.
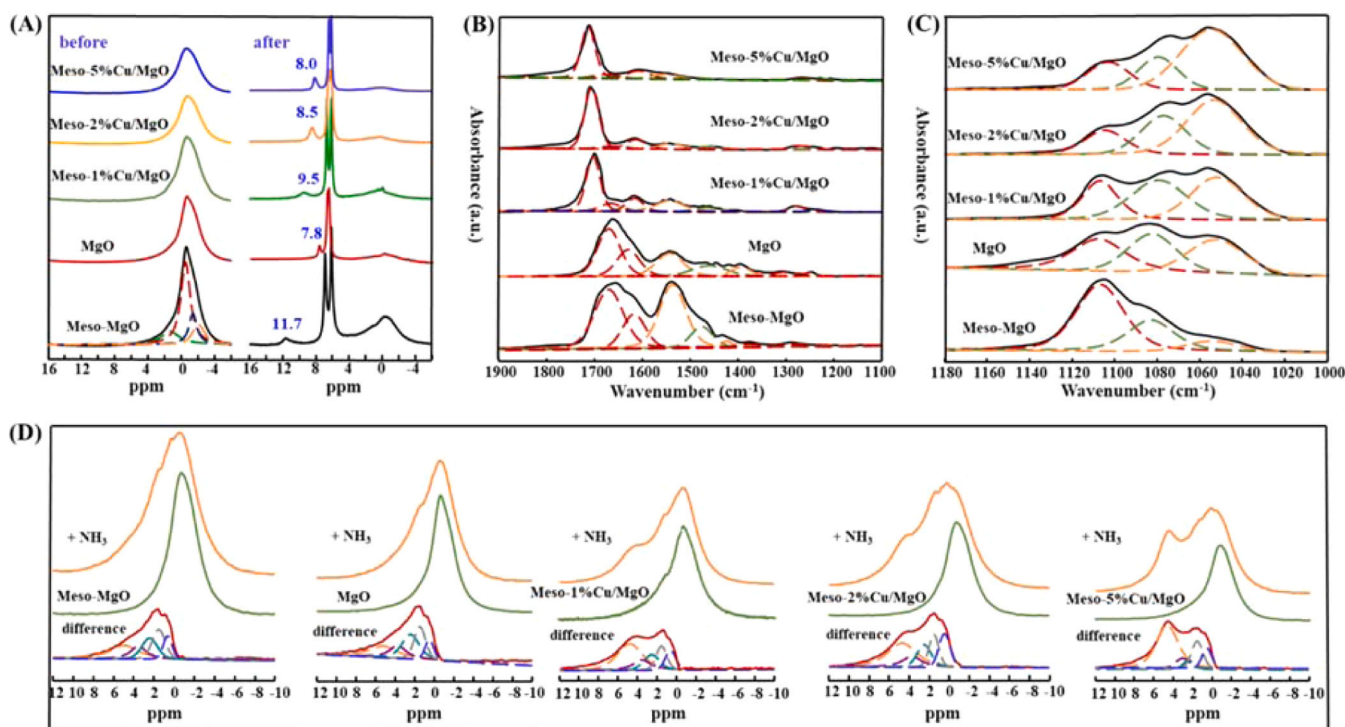
Fig. 5. (A) ^{1}H MAS NMR spectra before and after pyrrole adsorption, (B) CO_2- (C) methanol-adsorbed IR spectra, (D) ^{1}H MAS NMR spectra before (green line) and after (orange line) NH_3 adsorption of Cu/MgO with different Cu loadings. The difference spectra (red line) were obtained by subtracting the spectra of dehydrated samples from the spectra after NH_3 adsorption.

correspond to the (111), (200), and (220) crystal planes of cubic MgO phase [52]. For the meso-MgO and meso-Cu/MgO, another diffraction peaks at 19.3 and 27.3° are also observed. This could be related to the reflection observed in the pattern of the MgO phase with hexagonal structure (https://next-gen.materialsproject.org/; mp-1190533). There is no obvious CuO phase after the impregnation of Cu due to low content. The textural properties of the samples were determined by N_2 physisorption. As shown in Fig. 4(C), both meso-MgO and meso-Cu/MgO possess dual hysteresis loops within the P/P_0 range of 0.4–0.8 and 0.8–1.0, which are attributed to the presence of a mesoporous structure and the aggregation of plate-like particles, respectively [52]. Density functional theory (DFT) method pore size distribution analysis shown in Fig. 4(D) reveals a mesopore size distribution for meso-Cu/MgO centered at ca. 3 nm (Table 1). The Brunauer-Emmett-Teller (BET) surface area and pore volume (Table 1) increase from 53 and 0.12 to 211 m^2/g and 0.34 cm^3/g, respectively, with the appearance of a mesoporous structure in meso-MgO compared to conventional MgO, and then decrease gradually after the addition of Cu, which further indicates that the addition of Cu could have a negative effect on the mesoporous structure of meso-MgO. The SEM images in Fig. S11 reveal a crystalline structure on the micron scale with a plate-like shape [53], which indirectly indicates that pores of 3 nm originated from the mesoporous sample itself, rather than the stacking pores between the particles.

3.4.2. Basicity and acidity characterizations

Fig. S12 shows the CO_2-TPD profiles of the composite catalysts of 2Mo-Fe-O combined with the conventional MgO or meso-Cu/MgO samples. The number of basic sites shown in Table 2 was estimated from the area under the corresponding CO_2-TPD curve. CO_2-TPD results show that 2Mo-Fe-O contains few basic sites and the combination of MgO increases the basic sites of the composite catalysts. In addition, meso-MgO has strong basic sites because the presence of the mesoporous structure would have more defects [47] and the addition of Cu decreases

both the amount and the strength of the basic sites over meso-MgO.

The differences in basic properties between the composite catalysts originate mostly from the diverse MgO due to the weak basicity of 2Mo-Fe-O. To avoid the dilution effect of 2Mo-Fe-O on the basicity characterizations and optimize the signal-to-noise ratio, we only conducted the following basicity characterizations for different MgO. ^{1}H MAS NMR experiments with pyrrole as the probe molecule were carried out to further verify the basic strengths of a series of meso-Cu/MgO samples. As shown in Fig. 5(A)-left, before the adsorption of pyrrole, ^{1}H MAS NMR spectra exhibit signals at ca. −2.1, −1.4, −0.5 and 1.3 ppm, corresponding to a wide distribution of various surface hydroxyl sites [54]. Three new peaks are observed after the adsorption of pyrrole, with intense peaks at around 6–7 ppm due to the protons of the aromatic pyrrole ring. The signal of the N-H group of pyrrole centered at 7.1 ppm in liquid pyrrole shows a larger chemical shift when it interacts with the basic sites and a larger ^{1}H chemical shift usually corresponds to the stronger basic strength [55,56]. As depicted in Fig. 5(A)-right, meso-MgO shows a peak centered at 11.7 ppm after the interactions between the N-H groups in pyrrole and the basic sites of meso-MgO. In the case of meso-1 %Cu/MgO, meso-2 %Cu/MgO, and meso-5 % Cu/MgO, the peaks shift to 9.5, 8.5, and 8.0 ppm, respectively, revealing that meso-MgO has the strongest basic strength and the modification of Cu would gradually decrease the basic strength of meso-MgO. For MgO, the peak shifts to 7.8 ppm, indicating the weak basicity of MgO. These ^{1}H MAS NMR results after pyrrole adsorption are in line with CO_2-TPD results.

The MgO samples contain O^{2-}, Mg^{2+}-O^{2-}, and OH groups, with strong, medium, and weak basicity, respectively [57]. They all have a deprotonation ability; thus, they could all activate isobutene for Prins condensation. Our experimental results combined with CO_2-TPD and ^{1}H MAS NMR after pyrrole adsorption show that weak basic sites in 2Mo-Fe-O are not effective in catalyzing Prins condensation, while meso-MgO with strong basic sites would lead to more CO_x produced. To further investigate which basic sites over MgO are friendly to Prins

Table 3
Acidic properties of the catalysts studied herein.

Catalysts	Total acidic sites (μmol/g)[a]	Acidic sites (%)[a]			Catalysts	Total NH_4^+/NH_3 at acid sites (μmol/g)[b]	NH_4^+ at Brönsted acid sites (μmol/g)[b]	NH_3 at Lewis acid sites (μmol/g)[b]
		Weak	Middle	Strong				
2Mo-Fe-O	4	1	2	1	-	-	-	
2Mo-Fe-O+MgO(3:2)	36	11	12	13	MgO	74	17	57
2Mo-Fe-O+meso-MgO(3:2)	29	6	5	18	Meso-MgO	63	15	48
2Mo-Fe-O+meso-1 %Cu/MgO(3:2)	52	13	25	14	Meso-1 %Cu/MgO	82	13	69
2Mo-Fe-O+meso-2 %Cu/MgO(3:2)	56	15	32	9	Meso-2 %Cu/MgO	94	18	76
2Mo-Fe-O+meso-5 %Cu/MgO(3:2)	66	10	32	24	Meso-5 %Cu/MgO	112	16	96

[a] measured by NH_3-TPD.
[b] measured by ^1H MAS NMR after NH_3 adsorption.

condensation, we conducted CO_2-adsorbed IR experiments, as these could be used to distinguish the types of basic sites through the different species formed after CO_2 adsorption [58]. As shown in Fig. 5(B), at least three different species are formed after CO_2 adsorption. The bands at around 1430 and 1530 cm^{-1} are assigned to unidentate carbonate formed over isolated surface O^{2-} ions after CO_2 adsorption. Bidentate carbonate formed on Mg^{2+}-O^{2-} pair sites show bands at about 1280–1380 cm^{-1} and 1620–1720 cm^{-1}. The formation of bicarbonate species involved surface hydroxyl groups, revealing bands at 1220 cm^{-1} as well as 1480 cm^{-1} [58,59]. We also quantitatively calculated the amount of three different species from the spectra shown in Fig. 5(B) and the results are listed in Table 2. It is found that the total amount of species formed over meso-MgO, especially the unidentate carbonate formed over O^{2-} after CO_2 adsorption is larger than over other catalysts, revealing the presence of significant amounts of O^{2-} sites over meso-MgO, corresponding to strong basic sites detected by CO_2-TPD and ^1H MAS NMR after pyrrole adsorption. The number of unidentate carbonate species decreases significantly after the addition of Cu while the CO_x selectivity gradually decreases with the amount of Cu increasing from 1 % to 2 %. These results further indicate that O^{2-} ions with strong basic strength are unfriendly to this reaction, aggravating the decomposition of methanol to produce CO_x. We found that, although the amount of O^{2-} over meso-1 %Cu/MgO and meso-2 %Cu/MgO is low, these sites maintain a high selectivity to isoprene, indicating that the basic strength of Mg^{2+}-O^{2-} and OH groups is strong enough to catalyze the Prins condensation but simultaneously not cause excessive methanol decomposition to produce CO_x. At this stage, it is not straightforward to accurately claim which basic site over MgO is the active site, because these three basic sites could activate isobutene. However, we could confirm that O^{2-} ions with a strong basic strength are not appropriate for this reaction. Thus, the addition of Cu decreased the amount of O^{2-} ions over meso-MgO and the basic sites of Mg^{2+}-O^{2-} and OH groups in 2Mo-Fe-O+meso-2 %Cu/MgO composite catalyst are sufficient to boost the activation of isobutene for Prins condensation. We hypothesize that Prins condensation could be carried out when Mg^{2+}-O^{2-} pairs are reduced and only OH groups exist because despite OH groups with a lower Brönsted basicity than O^{2-}, they still exhibit high reactivity in some reactions [60,61].

We further studied the state of methanol by FT-IR after the adsorption of methanol. The amount of dissociated methanol obtained through the integrated area of ν_{C-O} band reveals the number of basic sites that could decompose methanol [57,62]. As shown in Fig. 5(C), the bands located at 1105 and 1076 cm^{-1} belong to monodentate methoxy and bidentate methoxy species, respectively, corresponding to the methanol in the dissociated state. The band centered at 1055 cm^{-1} is assigned to molecularly adsorbed methanol [57]. Methanol in dissociated state would further decompose to produce CO_x over basic sites or dimethyl ether over acidic sites [43], which are undesired routes for methanol

oxidization. The integrated area of the ν_{C-O} band shown in Table 2 was used to quantify the amount of methanol decomposed. We found that most of the methanol molecules are dissociated over meso-MgO and only a few methanol molecules are preserved, indicating that methanol over the meso-MgO surface would easily decompose to CO_x, in line with the experimental results where the catalyst 2Mo-Fe-O+meso-MgO (3:2) gives higher amounts of CO_x as compared to other catalysts. The amount of dissociated methanol decreases gradually with the Cu content from 1 % to 5 %, indicating that the addition of Cu decreases the amount and weakens the strength of the basic sites; thus, inhibiting the decomposition of methanol. Large amounts of basic sites over MgO lead to the formation of CO_x, and the weak base strength of MgO also inevitably weakens Prins condensation, resulting in the formation of more CO_x produced through HCHO over-oxidation. Strong basic strength or too many basic sites would decompose methanol to CO_x, resulting in lower methanol oxidation rates. Conversely, it would weaken the competitiveness of Prins condensation relative to HCHO over-oxidation. H_2-TPR (Fig. S13) and TPSR of methanol (Fig. S14) over different samples reveal that the presence of CuO in meso-5 %Cu/MgO may lead to the over oxidation of methanol to produce more CO_x.

We also investigated the acidic properties of the samples because the acid sites could also catalyze the Prins condensation. In addition, the presence of acid sites could provide adsorption sites for the reactants and intermediate products and catalyze the dehydration of isoprenol to isoprene, thus facilitating the reaction. The acidic properties of the catalysts were evaluated through NH_3-TPD and ^1H MAS NMR after NH_3 adsorption. NH_3-TPD profiles (Fig. S15, Table 3) reveal that 2Mo-Fe-O has low amounts of acidic sites. The number of total acid sites, especially the weak and medium strength acidic sites of 2Mo-Fe-O+meso-Cu/MgO (3:2), increases gradually with the increase of Cu content.

To further determine the role of the Brönsted and Lewis acidic sites on the catalyst surfaces, an ^1H MAS NMR investigation of the samples after NH_3 adsorption was conducted. The difference spectra were obtained by subtracting the spectra of the dehydrated samples from the spectra after NH_3 adsorption (Fig. 5(D)). All the samples show new peaks centered at around 0–5 ppm, indicating that these catalysts all have weak Brönsted acid sites and different Lewis acid sites [55,63,64]. The peaks centered at 4.8, 2.5, 1.3, and 0.4 ppm are assigned to NH_3 adsorbed on Lewis acid sites [55,63–65], while the signals centered at 3.5–3.7 ppm indicate the presence of Mg-OH with weak Brönsted acid property [55,64]. After the modification of meso-MgO with Cu, the intensities of the acid sites, especially the Lewis acid sites centered at 4.8 ppm increase with the Cu content increasing from 1 % to 5 %. Furthermore, the intensity of Brönsted acid sites centered at 3.5–3.7 ppm decreases slightly with the Cu loading, which is possibly due to the aggregation of OH groups on the meso-MgO surface after addition of Cu.

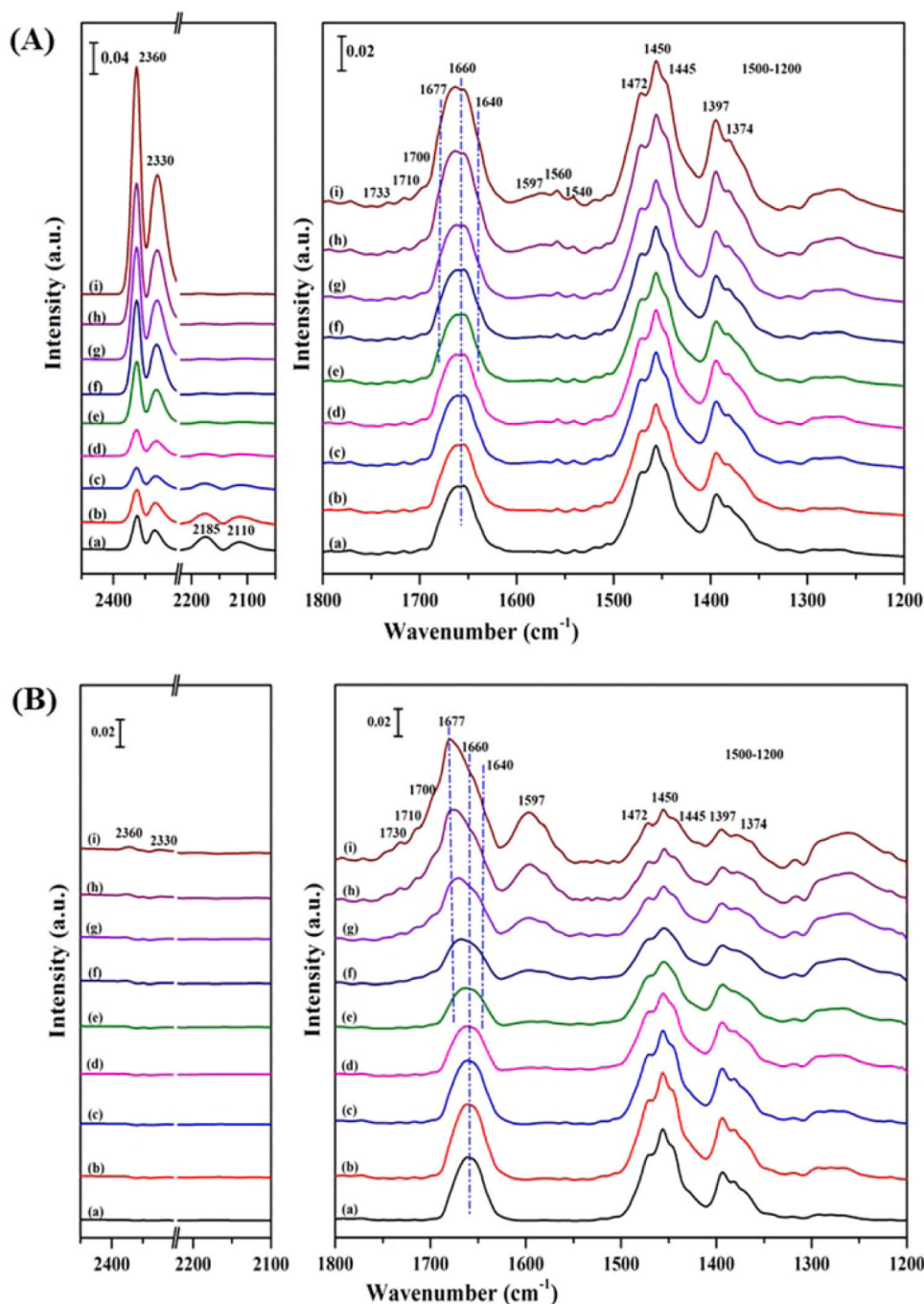By correlating the basicity/acidity characterizations with the

Fig. 6. *In-situ* DRIFT spectra of methanol and isobutene co-adsorption and reaction at 2.0 MPa over (A) 2Mo-Fe-O and (B) 2Mo-Fe-O+meso-2 %Cu/MgO(3:2) composite catalysts at (a) 100, (b) 120, (c) 140, (d) 160, (e) 180, (f) 200, (g) 220, (h) 240 and (i) 260 ℃.

catalytic performances, it is clear that the catalyst basicity/acidity play a vital role in highly selective production of isoprene via oxidative Prins reaction. The basicity/acidity of 2Mo-Fe-O is insufficient to efficiently catalyze the Prins condensation between formaldehyde and isobutene, resulting in excessive oxidation of HCHO to CO_x. The selectivity of isoprene increases obviously on the composite 2Mo-Fe-O+MgO catalyst compared to 2Mo-Fe-O catalyst, which indicates the increase of the strength and the number of basic sites, activate isobutene and thus improve the Prins condensation and prevent the over-oxidation of formaldehyde. However, 2Mo-Fe-O+meso-MgO (3:2) gives more CO_x than 2Mo-Fe-O+MgO (3:2), and adding appropriate amount of Cu decreases the CO_x selectivity (Fig. 3). According to the basicity characterization shown in Fig. 5(A-C), strong basicity and excessive number of

basic sites would decompose methanol or HCHO to produce CO_x, resulting in the decrease of isoprene selectivity. 2Mo-Fe-O+meso-2 % Cu/MgO with a proper number of basic sites and middle basic strength results in ca. 85 % selectivity to isoprene with only less 10 % selectivity to CO_x. In addition, the increase of middle acid sites and Lewis acid sites after addition of Cu would supply adsorption sites for reactants and benefit the dehydration of isoprenol to isoprene.

3.5. Reaction pathways of methanol and isobutene to isoprene

In-situ DRIFTS of methanol and isobutene adsorption were performed to better understand the surface species and reaction network of the oxidative Prins reaction. The IR studies of methanol chemisorption on
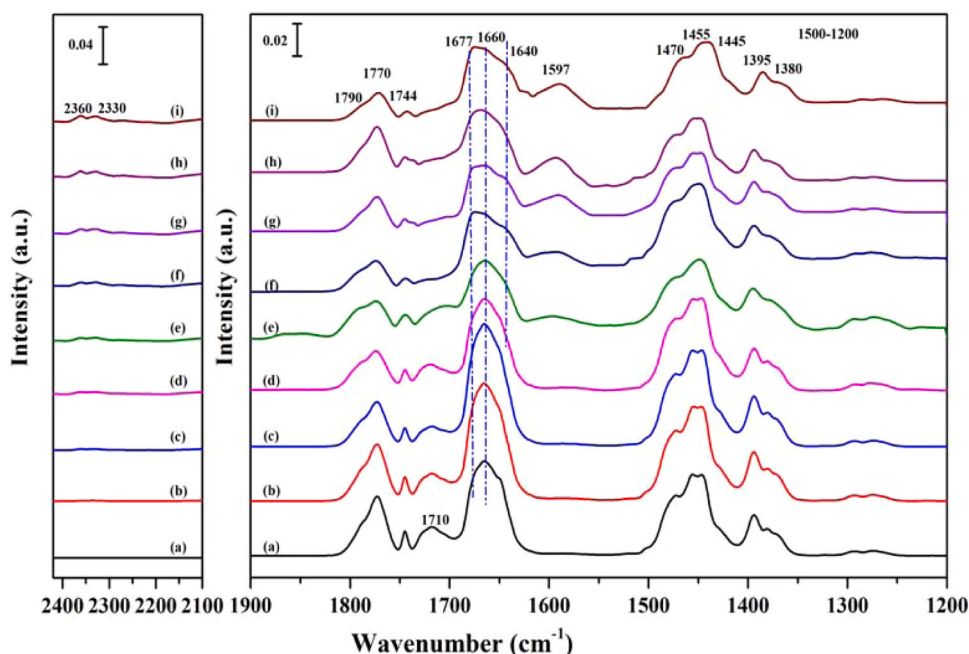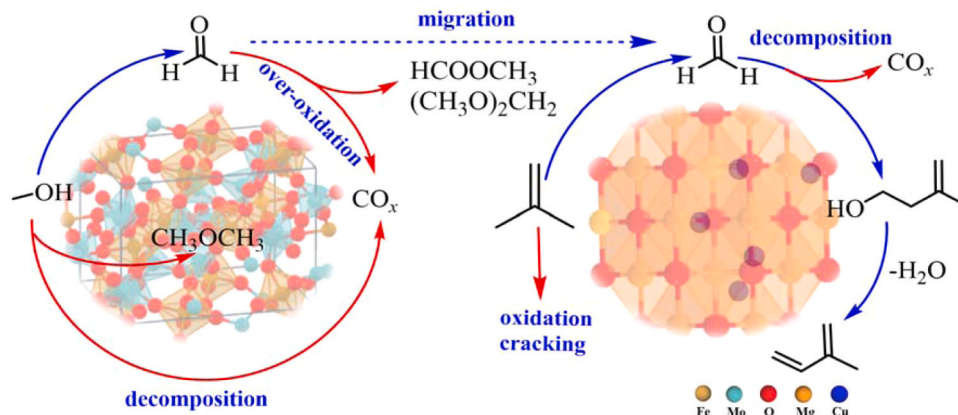
Fig. 7. *In-situ* DRIFT spectra of formaldehyde and isobutene co-adsorption and reaction at 2.0 MPa over 2Mo-Fe-O+meso-2 %Cu/MgO(3:2) composite catalysts at (a) 100, (b) 120, (c) 140, (d) 160, (e) 180, (f) 200, (g) 220, (h) 240 and (i) 260 ℃.

2Mo-Fe-O+meso-2 %Cu/MgO composite catalysts in Fig. S16(A) shows that the adsorbed methanol and methoxy species will transform to produce HCHO [35], supplying HCHO for the following Prins condensation with isobutene. In addition, the CO and formate species detected indicate that the over-oxidation of formaldehyde occurred and it is a parallel and competitive reaction to Prins condensation as illustrated in the above work. Studies of the surface species of isobutene reaction on 2Mo-Fe-O+meso-2 %Cu/MgO(3:2) composite catalysts shown in Fig. S16(B) indicate that the side reactions of isobutene alone is very weak.

The reaction processes of methanol and isobutene over 2Mo-Fe-O and 2Mo-Fe-O+meso-2 %Cu/MgO(3:2) composite catalysts are compared. The co-adsorption and reaction of methanol and isobutene over 2Mo-Fe-O catalyst is shown in Fig. 6(A), the peak observed at 1660 cm^{-1} is the typical signal of the C=C stretching of isobutene [66] and those due to CH deformation vibrations are observed at around 1500–1200 cm^{-1} typically at 1472, 1450, 1445, 1397 and 1374 cm^{-1} [67]. The bands at ~ 1677, 1700, 1710 and 1733 cm^{-1} are assigned to the C=O vibration of HCHO [68–71], indicating the formation of HCHO through methanol oxidation. The bands at 1560 and 1540 cm^{-1} are

assigned to HCOO$^-$ species [69,70]. Apparently two strong IR peaks at ~ 2360 and 2330 cm^{-1} are detected, which are associated with the P and R branches of asymmetrical vibration in CO$_2$ [72,73]. The weak bands at 2185 and 2110 cm^{-1} indicate the minor amounts of CO produced [74]. The vibrations at ~1640 and 1597 cm^{-1} can be assigned to C=C bands of isoprenol and isoprene [75,76], respectively, indicating that the Prins condensation between HCHO and isobutene to isoprenol and then the dehydration to isoprene occur with increasing reaction temperatures. Large amount of CO$_x$ while little isoprenol and isoprene are detected in Fig. 6(A), indicating the over-oxidation of HCHO is intense over individual 2Mo-Fe-O catalyst, which is consistent with the catalytic performance as shown in Fig. 1. This further demonstrates that the generated HCHO from methanol over 2Mo-Fe-O catalyst should undergo Prins condensation with isobutene immediately in order to ensure the formation of isoprene, which is closely related to the basicity/acidity of the catalyst. Fig. 6(B) shows the in-situ IR spectra of methanol and isobutene on the 2Mo-Fe-O+meso-2 %Cu/MgO composite catalysts. Compared with the results obtained over 2Mo-Fe-O, the retained HCHO, minor CO$_x$ and much more isoprenol and isoprene are detected, demonstrating that the combination of meso-2 %Cu/MgO with

Scheme 1. Possible main reaction pathways for methanol and isobutene to isoprene over composite catalysts.
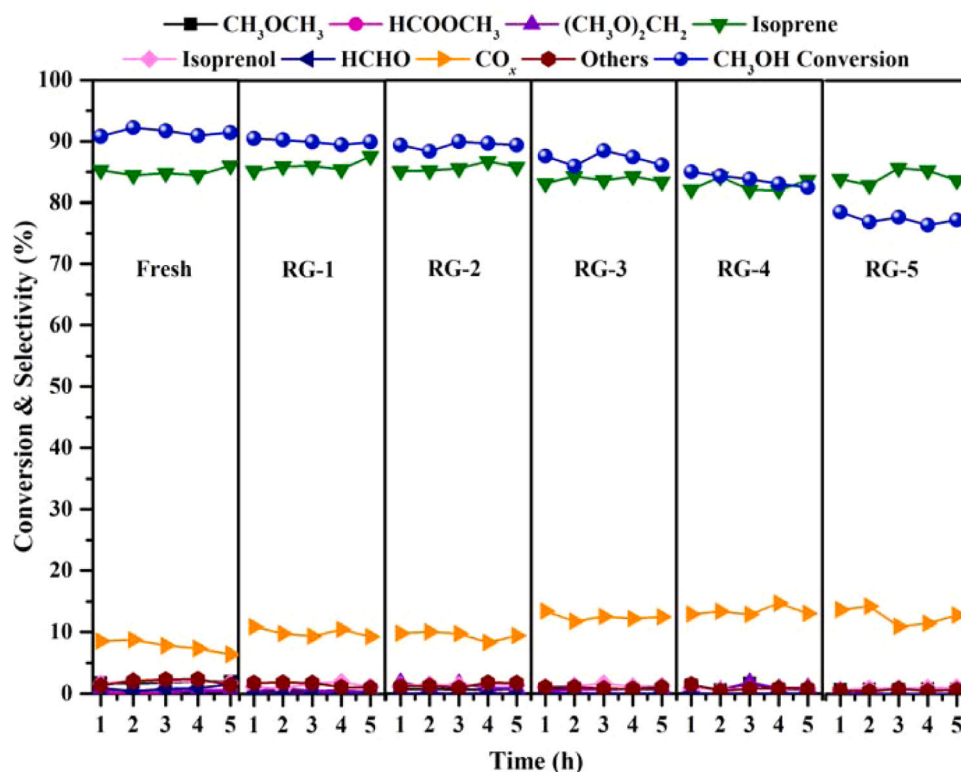
Fig. 8. Catalytic performances of the spent 2Mo-Fe-O+meso-2 %Cu/MgO (3:2) catalyst after successive regeneration cycles.

2Mo-Fe-O inhibits the over-oxidation of HCHO and boosts the Prins condensation between HCHO and isobutene efficiently.

The in-situ DRIFTS experiments of HCHO and isobutene co-adsorption and reaction were also carried out over 2Mo-Fe-O+meso-2 %Cu/MgO catalysts to further study the Prins condensation process. The individual HCHO adsorption over 2Mo-Fe-O+meso-2 %Cu/MgO is shown in Fig. S16(C). The bands at 1770–1790 cm^{-1} are assigned to the

C═O of formic acid [77]. The bands at 1677, 1710, 1730 and 1744 cm^{-1} are assigned to the C═O of formaldehyde [68,70,71]. The intensities of CO_x increase with the temperature in Fig. S16(C), indicating the over-oxidation and the decomposition of HCHO over 2Mo-Fe-O and meso-2 %Cu/MgO. However, after introducing isobutene on the catalysts as shown in Fig. 7 the bands centered at 1640 and 1597 cm^{-1} corresponding to isoprenol and isoprene, respectively, increase gradually
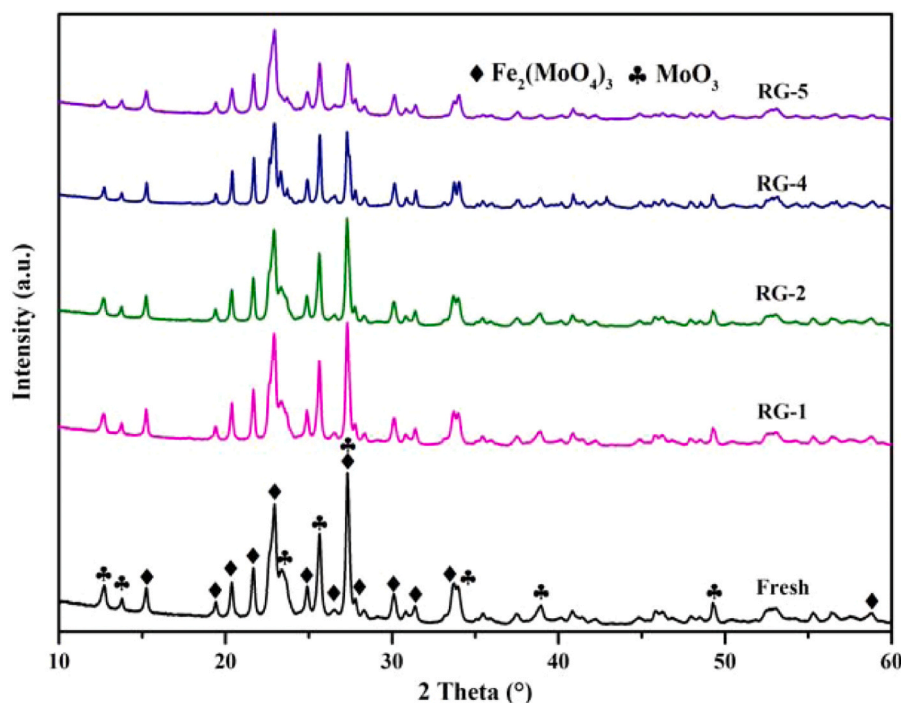

Fig. 9. XRD patterns of the 2Mo-Fe-O before and after re-usability tests.
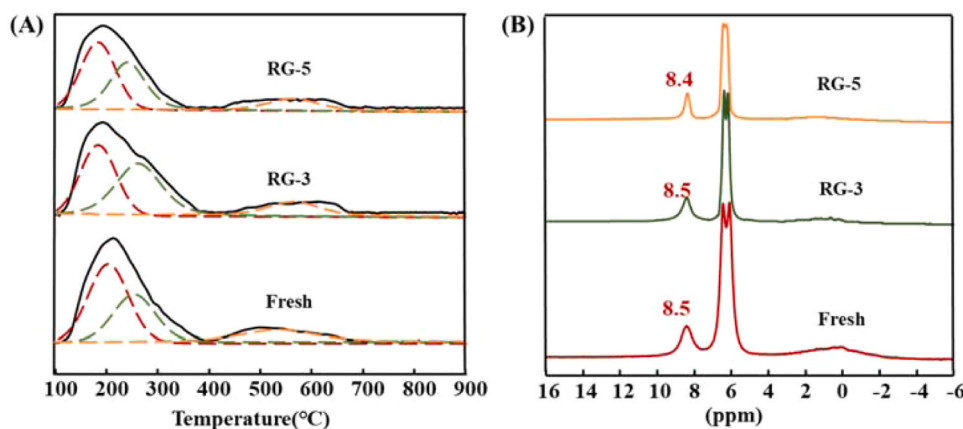
Fig. 10. CO$_2$-TPD profiles (A), ^{1}H MAS NMR spectra (B) after pyrrole adsorption of the recycled meso-2 %Cu/MgO catalyst.

with increasing the reaction temperatures. In the mean time, minor CO$_2$ and CO detected in Fig. 7 also illustrates the Prins condensation occurs between HCHO and isobutene.

To summarize the above discussion, the possible reaction pathways for the oxidative Prins reaction between methanol and isobutene are proposed in Scheme 1. HCHO produced in-situ from methanol oxidation over 2Mo-Fe-O migrates to the surface of MgO and immediately undergoes Prins condensation with the activated isobutene, producing isoprenol and then isoprene through dehydration. While the over-oxidation or decomposition of HCHO and methanol over the basic sites would produce CO$_x$ as discussed above, which would hinder the production of formaldehyde or consume generated formaldehyde; thus, further weakening the Prins condensation, which is closely related to the balance of oxidation and base-acid properties of the composite catalysts.

3.6. Recycle capability and stability of Mo-Fe-O+meso-Cu/MgO catalysts

Catalyst re-usability and stability are very important for practical applications. As shown in Fig. 8, both methanol conversion and isoprene selectivity are properly restored over 2Mo-Fe-O+meso-2 %Cu/MgO (3:2) after three successive regeneration cycles. CH$_3$OH conversion decreases from ca. 91 to 78 % while the selectivity of isoprene remains as high as 85 % after five successive regeneration cycles. Active sites for methanol oxidation over Mo-Fe-O have been previously identified to be Fe$_2$(MoO$_4$)$_3$ and MoO$_3$ phases, and the presence of excess crystalline MoO$_3$ in the bulk iron molybdate catalyst enhances the catalytic performance during the selective methanol oxidation reaction [29,35]. In addition, the presence of excess crystalline MoO$_3$ is necessary to replenish the surface MoO$_x$ lost by volatilization during methanol oxidation [35]. XRD characterization in Fig. 9 indicates that the relative intensities of the active sites Fe$_2$(MoO$_4$)$_3$ and MoO$_3$ for methanol oxidation decrease gradually after successive regeneration cycles. This possibly results in the lower methanol oxidation rates.

The basicity of meso-2 %Cu/MgO before and after recycle test was also measured by CO$_2$-TPD and ^{1}H MAS NMR after the adsorption of pyrrole (Fig. 10). The amounts of basic sites are provided in Table S2. The total quantity of basic sites decreases gradually from 445 to 400 µmol/g after five consecutive recycles, and the strong basic sites decreased from 75 to 40 µmol/g. ^{1}H MAS NMR after pyrrole adsorption in Fig. 10(B) illustrates that there is no discernible difference in the basic strength of meso-2 %Cu/MgO before and after recycles. Combined with the catalytic performances shown in Fig. 8, we deduce that there is a decrease in the amount of Fe$_2$(MoO$_4$)$_3$ and MoO$_3$ phases during the recycle process, which leads to the decrease in methanol conversion. This also indicates the importance of oxidative sites in the first step of the oxidative Prins reaction. Although the amount and distribution of meso-2 %Cu/MgO change slightly during recycle test, the remaining

basic sites are still sufficient to ensure Prins condensation, and the selectivity for isoprene can keep almost unchanged.

We further increased the reaction time to 55 h to test the stability of the 2Mo-Fe-O+meso-2 %Cu/MgO (3:2) composite catalysts. As shown in Fig. S17, methanol conversion remains at around 91–88 %, and isoprene selectivity keeps almost stable at 85 % during 55 h of time on stream. This demonstrates the composite catalysts have relatively high stability.

4. Conclusions

Composite catalysts containing a mixture of Mo-Fe oxide and meso-Cu/MgO with oxidation and basic/acidic sites can catalyze oxidative Prins reaction of methanol and isobutene to isoprene with high selectivity. The oxidation characteristics of Mo-Fe oxide are required for the in-situ production of HCHO, while HCHO and isobutene are subsequently activated through Prins condensation to isoprene over basic/acidic sites. We demonstrate that 2Mo-Fe-O+meso-2 %Cu/MgO (3:2) composite catalysts with balanced basicity and acidity can generate 91 % methanol conversion and 85 % isoprene selectivity under optimized reaction conditions. CO$_2$-TPD, ^{1}H MAS NMR after pyrrole adsorption, and the methanol-adsorbed and CO$_2$-adsorbed FT-IR spectra reveal that a proper amount of basic sites with medium strength are required to provide high isoprene selectivity, while strong basic sites such as O^{2-} leads to the decomposition of methanol to CO$_x$. NH$_3$-TPD and ^{1}H MAS NMR after NH$_3$ adsorption indicate that the addition of Cu decreases the number of O^{2-} ions, thereby increasing the number of middle acidic sites and Lewis acid sites. As a result, the isoprene selectivity is improved. The in-situ DRIFTS experiments suggest that the possible reaction pathways of oxidative Prins condensation over 2Mo-Fe-O+meso-2 %Cu/MgO composite catalysts could be: methanol→formaldehyde→ isoprenol→isoprene. The 2Mo-Fe-O+meso-2 %Cu/MgO (3:2) composite catalysts also show good re-usability and stability, with the selectivity to isoprene remaining as high as 85 % after five consecutive recycles.

CRediT authorship contribution statement

Lulu Xu: Experiments, Data analysis, Data curation, Writing – original draft preparation and revision. **Shuo Liu:** Investigation, Data analysis. **Weiping Zhang:** Conceptualization, Methodology, Supervision, Funding acquisition, Writing – review & editing. All other authors provided critical feedback and helped shape the research, data analysis and manuscript.

Declaration of Competing Interest

The authors have filed patents on the catalysts described in this

work.

Data availability

Data will be made available on request.

Acknowledgements

We thank Dr. Eduard Kunkes of BASF SE, Germany for the helpful discussion and suggestions. This work was supported by the INCOE (International Network of Centers of Excellence) project coordinated by BASF SE, Germany. The supports from the National Natural Science Foundation of China (No. 21673027, 21872017) were also acknowledged.

Appendix A. Supporting information

Supplementary data associated with this article can be found in the online version at doi:10.1016/j.apcatb.2023.123341.

References

[1] A.R.C. Morais, S. Dworakowska, A. Reis, L. Gouveia, C.T. Matos, D. Bogdał, R. Bogel-Łukasik, Chemical and biological-based isoprene production: green metrics, Catal. Today 239 (2015) 38–43.
[2] L. Zhang, T. Suzuki, Y. Luo, M. Nishiura, Z. Hou, Cationic alkyl rare-earth metal complexes bearing an ancillary bis (phosphinophenyl) amido ligand: a catalytic system for living cis-1,4-polymerization and copolymerization of isoprene and butadiene, Angew. Chem. Int. Ed. 46 (2007) 1909–1913.
[3] M. Zimmermann, K.W. Tornroos, R. Anwander, Cationic rare-earth-metal half-sandwich complexes for the living trans-1,4-isoprene polymerization, Angew. Chem. Int. Ed. 47 (2008) 775–778.
[4] I. Ivanova, V.L. Sushkevich, Y.G. Kolyagin, V.V. Ordomsky, Catalysis by coke deposits: synthesis of isoprene over solid catalysts, Angew. Chem. Int. Ed. 125 (2013) 13199–13202.
[5] G.O. Ezinkwo, V.F. Tretjakov, R.M. Talyshinky, A.M. Ilolov, T.A. Mutombo, Overview of the catalytic production of isoprene from different raw materials: propects of isoprene production from bio-ethanol, Catal. Sustain. Energy 1 (2013) 100–111.
[6] C.-T. Wu, K.M.K. Yu, F. Liao, N. Young, P. Nellist, A. Dent, A. Kroner, S.C.E. Tsang, A non-syn-gas catalytic route to methanol production, Nat. Commun. 3 (2012) 1050.
[7] P. Gautam, Neha, S.N. Upadhyay, S.K. Dubey, Bio-methanol as a renewable fuel from waste biomass: current trends and future perspective, Fuel 273 (2020), 117783.
[8] A. Saaret, B. Villiers, F. Stricher, M. Anissimova, M. Cadillon, R. Spiess, S. Hay, D. Leys, Directed evolution of prenylated FMN-dependent Fdc supports efficient in vivo isobutene production, Nat. Commun. 12 (2021) 5300.
[9] S. Sherkhanov, T.P. Korman, S. Chan, S. Faham, H. Liu, M.R. Sawaya, W.-T. Hsu, E. Vikram, T. Cheng, J.U. Bowie, Isobutanol production freed from biological limits using synthetic biochemistry, Nat. Commun. 11 (2020) 4292.
[10] Z. Zhang, Y. Wang, J. Lu, C. Zhang, M. Wang, M. Li, X. Liu, F. Wang, Conversion of isobutene and formaldehyde to diol using praseodymium-doped CeO₂ catalyst, ACS Catal. 6 (2016) 8248–8254.
[11] X. Yu, Y. Zhang, B. Liu, H. Ma, Y. Wang, Q. Bao, Z. Wang, Effect of phosphoric acid on HZSM-5 catalysts for Prins condensation to isoprene from isobutylene and formaldehyde, Chem. Res. Chin. Univ. 34 (2018) 485–489.
[12] V.L. Sushkevich, V.V. Ordomsky, I.I. Ivanova, Synthesis of isoprene from formaldehyde and isobutene over phosphate catalysts, Appl. Catal. A: Gen. 441–442 (2012) 21–29.
[13] V.L. Sushkevich, V.V. Ordomsky, I.I. Ivanova, Isoprene synthesis from formaldehyde and isobutene over Keggin-type heteropolyacids supported on silica, Catal. Sci. Technol. 6 (2016) 6354–6364.
[14] E. Dumitriu, D. Trong On, S. Kaliaguine, Isoprene by Prins condensation over acidic molecular sieves, J. Catal. 170 (1997) 150–160.
[15] O.A. Ponomareva, D.L. Chistov, P.A. Kots, V.R. Drozhzhin, L.I. Rodionova, I.I. Ivanova, Isoprene synthesis from formaldehyde and isobutylene in the presence of aluminum-and niobium-containing BEA catalysts, Petrol. Chem. 60 (2020) 942–949.
[16] H. Zhu, R. Zhang, Q. Wang, S. Xu, Insighting into the effect of acid sites on the catalytic performance of HZSM-5 during the one-step preparation of isoprene by formaldehyde and isobutene, Catal. Lett. 151 (2020) 435–444.
[17] W. Dai, C. Wang, X. Yi, A. Zheng, L. Li, G. Wu, N. Guan, Z. Xie, M. Dyballa, M. Hunger, Identification of tert-butyl cations in zeolite H-ZSM-5: evidence from NMR spectroscopy and DFT calculations, Angew. Chem. Int. Ed. 54 (2015) 8783–8786.
[18] S. Wang, E. Iglesia, Mechanism of isobutanal–isobutene Prins condensation reactions on solid Brønsted acids, ACS Catal. 6 (2016) 7664–7684.

[19] D. Mores, J. Kornatowski, U. Olsbye, B.M. Weckhuysen, Coke formation during the methanol-to-olefins conversion: in situ microspectroscopy on individual HZSM-5 crystals with different Brönsted acidity, Chem. -Eur. J. 17 (2011) 2874–2884.
[20] Y. Li, D. Sun, X. Zhao, Y. Yamada, S. Sato, Control of coke deposition in solid acid catalysis through the doping of transition metal combined with the assitance of H₂: a review, Appl. Catal. A 626 (2021), 118340.
[21] Y. Sun, L. Wei, Z. Zhang, H. Zhang, Y. Li, Coke formation over zeolite catalysts in light alkanes aromatization and anti-carbon-deposition strategies and perspectives: a review, Energy Fuels 37 (2023) 1657–1677.
[22] S.P. Bedenko, A.A. Kozhevnikov, K.I. Dement'ev, V.F. Tret'yakov, A.L. Maximov, The Prins condensation between i-butene and formaldehyde over modified BEA and MFI zeolites in liquid phase, Catal. Commun. 138 (2020), 105965.
[23] T. Okachi, M. Onaka, Formaldehyde encapsulated in zeolite: a long-lived, highly activated one-carbon electrophile to carbonyl-ene reactions, J. Am. Chem. Soc. 126 (2004) 2306–2307.
[24] C. Zuo, T. Ge, X. Guo, C. Li, S. Zhang, Synthesis and catalytic performance of Cs/P modified ZSM-5 zeolite in aldol condensation of methyl acetate with different sources of formaldehyde, Microporous Mesoporous Mater. 256 (2018) 58–66.
[25] X. Tang, Y. Bai, A. Duong, M.T. Smith, L. Li, L. Zhang, Formaldehyde in China: production, consumption, exposure levels, and health effects, Environ. Int. 35 (2009) 1210–1224.
[26] Y. Song, Y. Wang, H. Zhu, P. Zhu, W. Cai, Strategy for the separation of the mixture of dimethyl carbonate, formaldehyde, and water, J. Chem. Eng. Data 66 (2021) 2606–2614.
[27] Y. Watanabe, Kobe, J. Kobayashi, T. Shi, Y. Toyoshima, N. Shi, M. Saito, I. Shi, Method for producing isoprene, US Patent 3574780(A), 1971.
[28] T. Matsumoto, H. Mlyake, K. Mlyshi, H. Kamiyama, Y. Tachlbama, Synthesis of isoprene from isobutene and Methanol over supported silver catalysts, J. Jpn. Petrol. Inst. 22 (1979) 142–147.
[29] P. Hellier, P.P. Wells, M. Bowker, Methanol oxidation over shell-core MOₓ/Fe₂O₃ (M= Mo, V, Nb) catalysts, Chin. J. Catal. 40 (2019) 1686–1692.
[30] C. Brookes, P.P. Wells, G. Cibin, N. Dimitratos, W. Jones, D.J. Morgan, M. Bowker, Molybdenum oxide on Fe₂O₃ core–shell catalysts: probing the nature of the structural motifs responsible for methanol oxidation catalysis, ACS Catal. 4 (2014) 243–250.
[31] B. Huang, C.H. Bartholomew, B.F. Woodfield, Improved calculations of pore size distribution for relatively large, irregular slit-shaped mesopore structure, Microporous Mesoporous Mater. 184 (2014) 112–121.
[32] G. Landi, P.S. Barbato, A. Di Benedetto, L. Lisi, Optimization of the preparation method of CuO/CeO₂ structured catalytic monolith for CO preferential oxidation in H₂-rich streams, Appl. Catal. B: Environ. 181 (2016) 727–737.
[33] M. Karatok, M.G. Sensoy, E.I. Vovk, H. Ustunel, D. Toffoli, E. Ozensoy, Formaldehyde selectivity in methanol partial oxidation on silver: effect of reactive oxygen species, surface reconstruction, and stability of intermediates, ACS Catal. 11 (2021) 6200–6209.
[34] K.-A. Thavornprasert, M. Capron, L. Jalowiecki-Duhamel, O. Gardoll, M. Trentesaux, A.-S. Mamede, G. Fang, J. Faye, N. Touati, H. Vezin, J.-L. Dubois, J.-L. Couturier, F. Dumeignil, Highly productive iron molybdate mixed oxides and their relevant catalytic properties for direct synthesis of 1, 1-dimethoxymethane from methanol, Appl. Catal. B: Environ. 145 (2014) 126–135.
[35] K. Routray, W. Zhou, C.J. Kiely, W. Grünert, I.E. Wachs, Origin of the synergistic interaction between MoO₃ and iron molybdate for the selective oxidation of methanol to formaldehyde, J. Catal. 275 (2010) 84–98.
[36] Z.Y. Dang, J.F. Gu, L. Yu, C.W. Zhang, Vapor-phase of isoprene from formaldehyde and isobutene over CuSO₄-MOₓ/SiO₂ catalysts, React. Kinet. Catal. Lett. 43 (1991) 495–500.
[37] A. Borowiec, A. Lilić, J.-C. Morin, J.-F. Devaux, J.-L. Dubois, S. Bennici, A. Auroux, M. Capron, F. Dumeignil, Acrolein production from methanol and ethanol mixtures over La-and Ce-doped FeMo catalysts, Appl. Catal. B: Environ. 237 (2018) 149–157.
[38] A. Lilic, S. Bennici, J.F. Devaux, J.L. Dubois, A. Auroux, Influence of catalyst acid/base properties in acrolein production by oxidative coupling of ethanol and methanol, ChemSusChem 10 (2017) 1916–1930.
[39] B.A. Williams, S.M. Babitz, J.T. Miller, R.Q. Snurr, H.H. Kung, The roles of acid strength and pore diffusion in the enhanced cracking activity of steamed Y zeolites, Appl. Catal. A: Gen. 177 (1999) 161–175.
[40] F. Jiao, J. Li, X. Pan, J. Xiao, H. Li, H. Ma, M. Wei, Y. Pan, Z. Zhou, M. Li, S. Miao, J. Li, Y. Zhu, D. Xiao, T. He, J. Yang, F. Qi, Q. Fu, X. Bao, Selective conversion of syngas to light olefins, Science 351 (2016) 1065–1068.
[41] L. Xu, R. Zhao, W. Zhang, One-step high-yield production of renewable propene from bioethanol over composite ZnCeOₓ oxide and HBeta zeolite with balanced Brönsted/Lewis acidity, Appl. Catal. B: Environ. 279 (2020) 119389.
[42] K. Cheng, B. Gu, X. Liu, J. Kang, Q. Zhang, Y. Wang, Direct and highly selective conversion of synthesis gas into lower olefins: design of a bifunctional catalyst combining methanol synthesis and carbon–carbon coupling, Angew. Chem. Int. Ed. 55 (2016) 4725–4728.
[43] T. Tsoncheva, L. Ivanova, C. Minchev, M. Fröba, Cobalt-modified mesoporous MgO, ZrO₂, and CeO₂ oxides as catalysts for methanol decomposition, J. Colloid Interface Sci. 333 (2009) 277–284.
[44] J.M. Lopez Nieto, E. Acosta Burga, G. Kremenic, Oxidation of isobutene over a silica-supported multicomponent oxide catalyst, Ind. Eng. Chem. Res. 29 (1990) 337–342.
[45] S.R.G. Carrazfin, C. Martfn, V. Rives, R. Vidal, Selective oxidation of isobutene to methacrolein on multiphasic molybdate-based catalysts, Appl. Catal. A: Gen. 135 (1996) 95–123.

[46] Y. Xiong, L.E. Cadus, L. Daza, P. Bertrand, J. Ladriere, P. Ruiz, B. Delmon, Solid-state reactivity of iron molybdate artificially contaminated by antimony ions and its relation with catalytic activity in the selective oxidation of isobutene to methacrolein, Top. Catal. 11 (2000) 167–180.

[47] W. Gao, T. Zhou, Q. Wang, Controlled synthesis of MgO with diverse basic sites and its CO_2 capture mechanism under different adsorption conditions, Chem. Eng. J. 336 (2018) 710–720.

[48] V. Hiremath, R. Shavi, J.G. Seo, Controlled oxidation state of Ti in MgO-TiO$_2$ composite for CO_2 capture, Chem. Eng. J. 308 (2017) 177–183.

[49] M. Badlani, I.E. Wachs, Methanol: a "smart" chemical probe molecule, Catal. Lett. 75 (2001) 3–4.

[50] F. Zaccheria, N.I. Shaikh, N. Scotti, R. Psaro, N. Ravasio, New concepts in solid acid catalysis: some opportunities offered by dispersed copper oxide, Top. Catal. 57 (2014) 1085–1093.

[51] S. Liu, X. Zhang, J. Li, N. Zhao, W. Wei, Y. Sun, Preparation and application of stabilized mesoporous MgO-ZrO$_2$ solid base, Catal. Commun. 9 (2008) 1527–1532.

[52] N.K. Nga, P.T.T. Hong, T.D. Lam, T.Q. Huy, A facile synthesis of nanostructured magnesium oxide particles for enhanced adsorption performance in reactive blue 19 removal, J. Colloid Interface Sci. 398 (2013) 210–216.

[53] F. Meshkani, M. Rezaei, Nickel catalyst supported on magnesium oxide with high surface area and plate-like shape: A highly stable and active catalyst in methane reforming with carbon dioxide, Catal. Commun. 12 (2011) 1046–1050.

[54] C. Chizallet, H. Petitjean, G. Costentin, H. Lauron-Pernot, J. Maquet, C. Bonhomme, M. Che, Identification of the OH groups responsible for kinetic basicity on MgO surfaces by ^{1}H MAS NMR, J. Catal. 268 (2009) 175–179.

[55] O.V. Larina, K.V. Valihura, T. Čendak, Effect of the cerium modification on acid–base properties of Mg–Al hydrotalcite-derived oxide system and catalytic performance in ethanol conversion, React. Kinet. Mech. Catal. 132 (2021) 359–378.

[56] X. Yi, G. Li, L. Huang, Y. Chu, Z. Liu, H. Xia, A. Zheng, F. Deng, An NMR scale for measuring the base strength of solid catalysts with pyrrole probe: a combined solid-state NMR experiment and theoretical calculation study, J. Phys. Chem. C 121 (2017) 3887–3895.

[57] M. Bailly, C. Chizallet, G. Costentin, J. Krafft, H. Lauronpernot, M. Che, A spectroscopy and catalysis study of the nature of active sites of MgO catalysts: thermodynamic Brønsted basicity versus reactivity of basic sites, J. Catal. 235 (2005) 413–422.

[58] D. Cornu, H. Guesmi, J.-M. Krafft, H. Lauron-Pernot, Lewis acido-basic interactions between CO_2 and MgO surface: DFT and DRIFT approaches, J. Phys. Chem. C. 116 (2012) 6645–6654.

[59] J.I. Di Cosimo, V.K. Díez, C. Ferretti, C.R. Apesteguía, Basic catalysis on MgO: generation, characterization and catalytic properties of active sites, Catalysis: RSC., London (2014) 1–28.

[60] F. Prinetto, G. Ghiotti, R. Durand, D. Tichit, Investigation of acid–base properties of catalysts obtained from layered double hydroxides, J. Phys. Chem. B 104 (2000) 11117–11126.

[61] J. Puriwat, W. Chaitree, K. Suriye, S. Dokjampa, P. Praserthdam, J. Panpranot, Elucidation of the basicity dependence of 1-butene isomerization on MgO/Mg (OH)$_2$ catalysts, Catal. Commun. 12 (2010) 80–85.

[62] C. Chizallet, M.L. Bailly, G. Costentin, H. Lauron-Pernot, J.M. Krafft, P. Bazin, J. Saussey, M. Che, Thermodynamic Brønsted basicity of clean MgO surfaces determined by their deprotonation ability: role of Mg^{2+}-O^{2-} pairs, Catal. Today 116 (2006) 196–205.

[63] J. Huang, N.V. Vegten, Y. Jiang, M. Hunger, A. Baiker, Increasing the Brønsted acidity of flame-derived silica/alumina up to zeolitic strength, Angew. Chem. Int. Ed. 49 (2010) 7776–7781.

[64] C. Wang, W. Dai, G. Wu, N. Guan, L. Li, Application of ammonia probe-assisted solid-state NMR technique in zeolites and catalysis, Magn. Reson. Lett. 2 (2022) 28–37.

[65] Q. Lei, C. Wang, W. Dai, G. Wu, N. Guan, M. Hunger, L. Li, Tandem Lewis acid catalysis for the conversion of alkenes to 1, 2-diols in the confined space of bifunctional TiSn-Beta zeolite, Chin. J. Catal. 42 (2021) 1176–1184.

[66] A.A. Gabrienko, Z.N. Lashchinskaya, S.S. Arzumanov, A.V. Toktarev, D. Freude, J. Haase, A.G. Stepanov, Isobutene transformation to aromatics on Zn-modified zeolite: particular effects of Zn^{2+} and ZnO species on the reaction occurrence revealed with solid-state NMR and FTIR spectroscopy, J. Phys. Chem. C 125 (2021) 15343–15353.

[67] A. Kogelbauer, J.G. Goodwin, Coadsorption of methanol and isobutene on HY zeolite, J. Phys. Chem. 99 (1995) 8777–8781.

[68] K. Liu, Z. Zhao, W. Lin, Q. Liu, Q. Wu, R. Shi, C. Zhang, H. Cheng, M. Arai, F. Zhao, N-methylation of N-methylaniline with carbon dioxide and molecular hydrogen over a heterogeneous non-noble metal Cu/TiO$_2$ catalyst, ChemCatChem 11 (2019) 3919–3926.

[69] N. Li, B. Huang, X. Dong, J. Luo, Y. Wang, H. Wang, D. Miao, Y. Pan, F. Jiao, J. Xiao, Z. Qu, Bifunctional zeolites-silver catalyst enabled tandem oxidation of formaldehyde at low temperatures, Nat. Commun. 13 (2022) 2209.

[70] M.D. Hernández-Alonso, I. Tejedor-Tejedor, J.M. Coronado, M.A. Anderson, J. Soria, Operando FTIR study of the photocatalytic oxidation of acetone in air over TiO$_2$-ZrO$_2$ thin films, Catal. Today 143 (2009) 364–373.

[71] S. Zhu, J. Zheng, S. Xin, L. Nie, Preparation of flexible Pt/TiO$_2$/γ-Al$_2$O$_3$ nanofiber paper for room-temperature HCHO oxidation and particulate filtration, Chem. Eng. J. 427 (2022), 130951.

[72] E.L. Force, A.T. Bell, Infrared spectra of adsorbed species present during the oxidation of ethylene over silver, J. Catal. 38 (1975) 440–460.

[73] R. Taylor, A. Pénicaud, N.J. Tower, Matrix isolation of fullerene-derived CO_2 at ambient temperature, Chem. Phys. Lett. 295 (1998) 481–486.

[74] C. Asokan, L. DeRita, P. Christopher, Using probe molecule FTIR spectroscopy to identify and characterize Pt-group metal based single atom catalysts, Chin. J. Catal. 38 (2017) 1473–1480.

[75] E. Ninnemann, G. Kim, A. Laich, B. Almansour, A.C. Terracciano, S. Park, K. Thurmond, S. Neupane, S. Wagnon, W.J. Pitz, S.S. Vasu, Co-optima fuels combustion: a comprehensive experimental investigation of prenol isomers, Fuel 254 (2019), 115630.

[76] Y. Ikushima, N. Satto, M. Arai, High-pressure fourier transform infrared spectroscopy study of the Diels-Alder reaction of isoprene and maleic anhydride in supercritical carbon dioxide, Bull. Chem. Soc. Jpn. 64 (1991) 282–284.

[77] L. Jia, D.A. Bulushev, S. Beloshapkin, J.R.H. Ross, Hydrogen production from formic acid vapour over a Pd/C catalyst promoted by potassium salts: evidence for participation of buffer-like solution in the pores of the catalyst, Appl. Catal. B: Environ. 160–161 (2014) 35–43.